

Stochastic Incentive-based Demand Response Program for Virtual Power Plant with Distributed Energy Resources

Pratik Harsh*, Hongjian Sun†, Debapriya Das‡, Awagan Goyal Rameshrao§, and Jing Jiang¶

Abstract—The growing integration of distributed energy resources (DERs) into the power grid necessitates an effective coordination strategy to maximize their benefits. Acting as an aggregator of DERs, a virtual power plant (VPP) facilitates this coordination, thereby amplifying their impact on the transmission level of the power grid. Further, a demand response program enhances the scheduling approach by managing the energy demands in parallel with the uncertain energy outputs of the DERs. This work presents a stochastic incentive-based demand response model for the scheduling operation of VPP comprising solar-powered generating stations, battery swapping stations, electric vehicle charging stations, and consumers with controllable loads. The work also proposes a priority mechanism to consider the individual preferences of electric vehicle users and consumers with controllable loads. The scheduling approach for the VPP is framed as a multi-objective optimization problem, normalized using the utopia-tracking method. Subsequently, the normalized optimization problem is transformed into a stochastic formulation to address uncertainties in energy demand from charging stations and controllable loads. The proposed VPP scheduling approach is addressed on a 33-node distribution system simulated using MATLAB software, which is further validated using a real-time digital simulator.

Index Terms—Demand response, Electric vehicles, Multi-objective optimization problem, Stochastic model, Virtual power plant.

NOMENCLATURE

Index and Sets

S^L	Set of nodes integrated with controllable loads.
S^N, n	Set and index denoting nodes of distribution network at which solar-powered generating station, charging station (CS), and battery swapping station (BSS) are integrated.
S^T, t	Set and index denoting operating intervals.

*Corresponding Author.

P. Harsh and H. Sun are with the Department of Engineering, Durham University, Durham, United Kingdom (e-mail: *pratik.harsh@durham.ac.uk; †hongjian.sun@durham.ac.uk).

D. Das is with the Department of Electrical Engineering, Indian Institute of Technology, Kharagpur, West Bengal 721302, India (e-mail: ‡ddas@ee.iitkgp.ac.in).

A. G. Rameshrao and J. Jiang are with the Department of Mathematics, Physics & Electrical Engineering, Northumbria University, Newcastle, United Kingdom (e-mail: §goyal.awagan@northumbria.ac.uk; ¶jing.jiang@northumbria.ac.uk).

This work was supported by the Engineering and Physical Sciences Research Council [grant number EP/Y005376/1] – VPP-WARD Project (<https://www.vppward.com>).

This work was also supported by the European Union's Horizon 2020 research and innovation programme under the Marie Skłodowska-Curie Grant Agreement No. 872172 TESTBED2 project.

\mathcal{S}^U, u	Set and index denoting uncertain input variables.
\mathcal{S}_B^n, b	Set and index denoting batteries at BSS of n^{th} node.
\mathcal{S}_V^n, v	Set and index denoting electric vehicles (EVs) at CS of n^{th} node.

Parameters

α^t	Market electricity price rate for power purchased from the utility grid (in \$/kWh).
β^n	Factor representing the discomfort due to load curtailment of the consumer connected to n^{th} node.
Δt	Operating hour in each interval (in h).
$\eta_{G2B/B2G}$	Battery charger efficiency during grid-to-battery (G2B)/battery-to-grid (B2G) mode.
$\eta_{G2V/V2G}$	EV charger efficiency during grid-to-vehicle (G2V)/vehicle-to-grid (V2G) mode.
$\lambda_{1/2}$	Limiting factors for load curtailments and solar generations, respectively.
μ_u, σ_u	Mean and standard deviation of the u^{th} uncertain input variable.
$(\underline{\cdot})/(\overline{\cdot})$	Lower/Upper boundary limit of the variable under bracket.
a_d, b_d	Coefficients of battery degradation.
c_b	Battery investment cost (in \$/kWh).
$c_{p/o}$	Annualized installation/maintenance cost coefficients of solar-powered generating station (in \$/kWp-year).
DB	Budget of distribution system (DS) operator (in \$).
$E_{v/b}^n$	Battery energy capacity of v^{th} EV or b^{th} battery connected to CS/BSS installed at n^{th} node (in kWh).
k_v, k_i	Voltage (in %V/ ⁰ C) and current (in %A/ ⁰ C) temperature coefficients of a solar module.
L^t	Lifetime of solar-powered station (in years).
m	Number of uncertain input variables.
$P_0^{n,t}$	Nominal power demand of consumer connected to n^{th} node at t^{th} operating interval (in kW).
$P_{s,rated}$	Nominal power rating of a solar module (in kWp).
r	Interest rate on investments for solar-powered station.
s^t	Solar irradiance at the t^{th} operating interval (in kW/m ²).
$SoC_{b,swap}^n$	State of charge (SoC) of EV registered to swap b^{th} battery connected to BSS installed at n^{th} node.
T	Total number of operating intervals.
$t_{b,arr}^n$	Arrival time of EV registered for swapping b^{th} battery connected to BSS installed at n^{th} node.
$T_{o/a}$	Nominal operating/ambient temperature (in ⁰ C).
$t_{start/stop}^n$	Start/stop time of load curtailment specified by consumer connected to n^{th} node.

$t_{v,dep}^n$	Departure time of v^{th} EV connected to CS installed at n^{th} node.
V_{MPP}, I_{MPP}	Solar module voltage (in V) and current (in A) at its maximum power point.
V_{OC}, I_{SC}	Open circuit voltage (in V) and short circuit current (in A) of a solar module.
w_i	Weighting factor accounting for the weightage of the individual objective function.
$z_{inj}^{n,t}$	Binary indicator to represent power injection from n^{th} node at t^{th} operating interval (+1, if power is injected to DS; 0, otherwise).
$z_{v/b}^{n,t}$	Operational mode indicator for v^{th} EV or b^{th} battery at t^{th} operating interval connected to CS/BSS installed at n^{th} node.

Variables

γ^t	Incentivised electricity price rate (in \$/kWh).
P_{grid}^t	Power delivery by the utility grid at t^{th} operating interval (in kW).
$P_{shift}^{n,t}$	Load shift of controllable loads connected to n^{th} node at t^{th} operating interval (in kW).
P_s^n	Capacity of solar-powered generating station installed at node n (in kWp).
$P_{v/b}^{n,t}$	Power demand of v^{th} EV or b^{th} battery at t^{th} interval connected to CS/BSS installed at n^{th} node (in kW).

I. INTRODUCTION

THE increasing concerns regarding climate change are driving the global trend towards decarbonization. However, despite a significant decline in global carbon emissions during the COVID-19 pandemic, emissions from energy sources promptly surged to their highest recorded levels by the end of 2021 [1]. The primary barrier challenging the modern power grid is shifting towards emission-less generation while ensuring reliable access to affordable energy. To enhance cleaner production and optimize energy consumption, modern power grids have been integrated with distributed energy resources (DERs) [2] and demand-side control and communications [3]. This integration empowers passive consumers to transition into proactive participants, referred to as prosumers [4], who actively oversee energy generation, storage, and consumption. However, individual prosumers exert minimal influence at the transmission level, and the intricate processing and communication infrastructure required for their market participation entails transaction costs that surpass potential gains. Additionally, fluctuations in market prices pose risks that are challenging to mitigate locally.

Effectively managing and coordinating DERs can yield various advantages for the power grid, including diminished network losses, alleviated transmission line congestion, peak demand reduction, heightened flexibility, and improved system resilience [5]–[7]. The concept of a virtual power plant (VPP), an aggregator of DERs including renewable sources, energy storage units, EVs, and controllable loads, has emerged to better coordinate the DERs enhancing their controllability, visibility, and influence in the transmission network [8]. Using a blend of hardware and software, VPPs not only facilitate access to a previously untapped utility-scale behind-the-meter

energy supply but also effectively manage geographically dispersed and diverse DERs to create unified demand-responsive assets [9]. Furthermore, a community-based VPP utilizing virtual islanding operations facilitates the sustainable energy transition of the distribution system [10], enabling it to integrate a higher proportion of renewable energy sources into the grid.

Various approaches have been suggested for coordinating DERs in VPPs, broadly categorized as direct and indirect approaches [11]. The direct approach allows the VPP operator to schedule DERs based on their operational requirements and users' priorities, thus ensuring predictable DER capacity and response and facilitating services requiring faster control, such as frequency regulation [12]–[14]. However, the processing and communication infrastructure needed for direct control might not be feasible for large VPPs. Moreover, the security and privacy issues associated with the direct methods raise significant concerns [15]. In an indirect approach, the individual prosumers have the freedom to schedule their flexible loads based on their priorities and the incentive signals sent by the VPP operator [16]–[18]. The indirect method can be employed by utilizing one-way signals, thereby diminishing communication needs and addressing privacy considerations. However, uniform pricing across multiple prosumers may lead to them all adjusting their energy consumption to coincide with low-price periods, potentially exacerbating demand peaks [19]. Additionally, employing indirect price-based coordination strategies could amplify demand fluctuations and compromise system stability [20]. Indirect coordination strategies prove advantageous when the expenses associated with communication infrastructure outweigh the benefits of a direct approach or when prosumers are reluctant to provide direct access to the VPP operator [21].

Furthermore, researchers have taken pioneering steps to integrate EV charge scheduling into VPP operations, aiming to enhance the support for sustainable developments. The widespread adoption of EVs presents new hurdles concerning grid integration and power system management. Uncoordinated EV charging patterns may cause significant spikes in electricity usage, potentially straining the power infrastructure, escalating costs, and compromising reliability [22]. Coordinated charging strategies have surfaced as efficient methods to mitigate the adverse effects of EVs on the distribution system (DS) [23]. Previous research in [24]–[26] has significantly advanced the integration of EVs into VPP operations as charging loads of DS. However, in practical scenarios, CSs serve as primary EV charging infrastructure providers [27], which help to address the challenges associated with integrating EVs as an individual unit in the DS. CSs possess the capacity to manage a larger quantity of charging units compared to individual household chargers, making them potential hubs for EV energy scheduling. Consequently, initial efforts have been undertaken to integrate CSs into VPP operations. A cooperative operation model has been proposed in [28] to maximize the benefit of the VPP-CSs system by considering the conflicting interests of different stakeholders. In [29], a Stackelberg game model has been presented to establish an interaction between CSs and VPP with renewables, thermal generators, and energy storage

units. A similar decentralized approach has been investigated in [30], in which CSs are operated based on the price signals set by VPP. Nevertheless, in these studies, the CSs are limited to reacting passively to VPP price signals rather than actively engaging with the VPP operator, potentially compromising the effectiveness of EVs as energy demand and storage units. In order to overcome this issue, centralized control to coordinate the CS energy scheduling with other elements of VPP has been presented in [31]. However, previous studies regarding the incorporation of EVs into VPP operations overlooked the priorities of EV users as an individual unit. This includes factors such as the preferred arrival and departure times of EV owners at the CSs, as well as the maximum amount of energy that can be delivered to them at their departure time. Moreover, with the introduction of fast EV chargers, the utility grid may experience an increase in the peak-to-average ratio of energy demand during the charging period of EVs. Consequently, effectively addressing the scheduling problem and maximizing the utilization of EVs at CSs as storage hubs has proven challenging.

The growing integration of unpredictable renewable sources and EVs within VPP introduces a continual risk associated with its engagement in the electricity market. In line with the imbalance market mechanism [32], VPPs bear responsibility for their supply discrepancies, which must be reconciled within the imbalance mechanism through costly alternatives. Consequently, substantial fluctuations in DERs can jeopardize the VPP's viability. Hence, it is crucial to devise a practical and effective strategy for VPPs to mitigate this risk. Historically, traditional power plants have been employed to act as the operational reserve, yet this approach demands substantial investment and exacerbates carbon emission concerns. Energy storage can potentially mitigate discrepancies in DER generation [33]; however, its feasibility is hindered by the current substantial upfront investment costs. Presently, leveraging smart technologies, demand response (DR) emerges as a cost-efficient strategy to address the aforementioned challenges [34]. From the perspective of the VPP, DR can be seen as a virtual operational reserve, aiding in offsetting deviations in DER generation. Generally, the DR program consists of two main categories: price-based DR and incentive-based DR. Price-based DR lacks dispatchability, resulting in reduced flexibility. Moreover, there is often a lack of consumer understanding regarding their electricity usage and billing, which prompts inquiries into whether participation in price-based DR programs is motivated by perceived savings rather than tangible savings [35]. Conversely, incentive-based DR offers the ability to dispatch resources and significantly greater flexibility in assisting the VPP in acquiring the necessary DR resources [36]. Hence, consumers are more inclined to engage in incentive-based DR programs than those based solely on pricing. Encouraging consumers to enroll in such incentive-based DR programs can enhance the stability of the VPP [37].

Furthermore, it is imperative to account for the uncertainties associated with renewable energy sources, electricity demand, and pricing when devising optimal scheduling strategies for VPPs. Various methodologies, such as robust, possibilistic, and stochastic optimization, have been examined in the literature

to analyze how uncertain variables affect the results of VPP scheduling problems [38]. Robust optimization is particularly applicable in scenarios where it is challenging to ascertain the distribution of uncertain parameters or when historical data is scarce in terms of both quantity and quality. Implementing robust optimization demands a clear understanding of uncertainty variables, encompassing their scale and extent, thereby presenting challenges in its application across specific power system problems [39], [40]. Alternatively, possibilistic [41] and stochastic [42] approaches quantify uncertain parameters by generating scenarios based on a membership function and probability density function (PDF), respectively, which are derived from historical data. Among these approaches, stochastic methods are comparatively simpler for power system issues. Stochastic techniques can additionally be categorized into analytical, numerical, and approximate methodologies. The analytical methods may sacrifice precision in calculating PDF of the uncertain input variable by employing simplifications such as linearizing system models and Gaussian distributions [43], [44]. Monte Carlo simulation is a widely employed and precise numerical method, particularly valued for its effectiveness in analyzing complex models with multiple random variables. This approach entails the generation of numerous random samples to represent uncertainties, thereby constructing a substantial dataset for assessing the PDFs of output parameters [45]. However, a drawback of numerical methods lies in the significant computational time needed to attain convergence. Nevertheless, approximate methods such as the point estimation method (PEM) provide a beneficial balance between precision and computational speed [46], [47]. This work explicitly adopts Hong's (2m+1) PEM [48] that utilizes deterministic approaches to tackle probabilistic concerns and alleviate obstacles arising from incomplete knowledge of probability distributions linked with random variables.

While extensive literature exists on the VPP scheduling problem, limited attention has been given to the challenges arising from the involvement of multiple stakeholders in VPP operations. Furthermore, as previously mentioned, there is a necessity to implement a priority-based energy scheduling strategy within the VPP scheduling framework, taking into account the preferences of EV owners and other energy consumers regarding their energy demand or load curtailment requirements. Following the identification of research gaps within the VPP scheduling problem, this study introduces a stochastic multi-objective energy scheduling problem modeled for the direct-controlled VPP. The main contributions of this work are listed below:

- 1) This work presents a multi-objective VPP scheduling problem aimed at maximizing the profit for the VPP operator while minimizing the installation costs of solar-powered generation stations, the expense of energy purchased from the grid, and the energy costs associated with CSs and controllable loads without compromising their energy requirements. Additionally, the proposed problem seeks to minimize EV battery degradation and consumer discomfort arising from V2G operations and load shifting, respectively. Furthermore, a stochastic

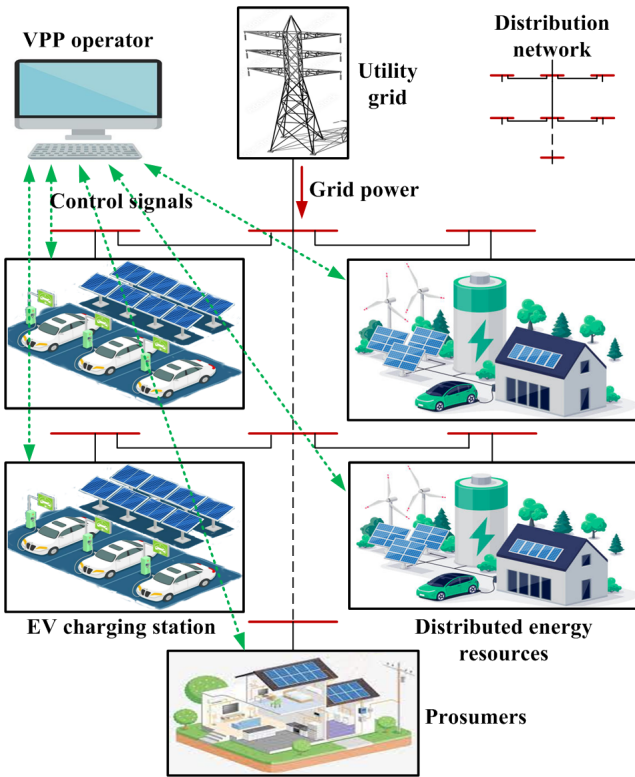


Fig. 1. Direct-controlled virtual power plant.

model of the proposed scheduling problem is presented to consider the uncertainties in the energy demand of EVs and controllable loads.

- 2) This work also integrates a priority mechanism within the mathematical model of EVs and consumers with controllable loads, considering their preferences during the scheduling operation. EVs prioritize achieving maximum SoC by the time they depart from CSs, while consumers with controllable loads aim to minimize energy consumption costs with minimal load shifting or curtailment.
- 3) An incentive-based DR program is proposed, which adopts a uniform incentivization approach to compensate controllable load owners for their inconvenience and EV users for their battery degradation. The incentivization mechanism guarantees that rewards for adjusting controllable loads and the V2G operation of EVs are allocated to DR participants based on a uniform incentive rate defined by the VPP operator.

II. MATHEMATICAL MODEL OF VPP

This section provides the mathematical model of solar-powered generating stations, EVs operating at CSs, batteries at BSSs, and controllable loads, that a VPP operator virtually aggregates through a direct-controlled approach. A schematic model of direct-controlled VPP, based on [11], is shown in Fig. 1.

A. Solar-powered generating station

The power output of solar-powered generating stations at each operating interval predominantly relies on the solar

TABLE I
OPERATIONAL MODE SELECTION MECHANISM FOR EV

$\rho_v^{n,t}$	≥ 1	Uncoordinated G2V mode ($z_v^{n,t} = 1$)	
	$p_v^{n,t}$	1	Coordinated G2V mode ($z_v^{n,t} = 0$)
0		0	Coordinated V2G mode ($z_v^{n,t} = -1$)

irradiance level and ambient temperature at the site, which can be expressed mathematically as [23]

$$P_s^{n,t} = \left[\frac{P_s^n}{P_{s,\text{rated}}} \right] \times FF \times V_s \times I_s, \quad \forall n \in \mathcal{S}^N; t \in \mathcal{S}^T \quad (1)$$

$$\text{where } FF = (V_{MPP}I_{MPP}) / (V_{OC}I_{SC}) \quad (1a)$$

$$V_s = V_{OC} - k_v T_c \quad (1b)$$

$$I_s = s^t (I_{SC} + k_i (T_c - 25)) \quad (1c)$$

$$T_c = T_a + s^t (T_o - 20) / 0.8 \quad (1d)$$

B. Electric vehicle charging station

EVs can be modeled as battery units when it is connected to the grid through CS for their charging operation. It can be represented using its state of charge (SoC), which is mathematically calculated as [23]

$$SoC_v^{n,t} = SoC_v^{n,t-1} + \eta_v (P_v^{n,t} \Delta t) / E_v^n, \\ \forall v \in \mathcal{S}_V^n; n \in \mathcal{S}^N; t \in \mathcal{S}^T \quad (2a)$$

$$\text{where } \eta_v = \begin{cases} \eta_{G2V}, & \text{if EV is in G2V mode} \\ 1/\eta_{V2G}, & \text{if EV is in V2G mode} \end{cases} \quad (2b)$$

It is important to note here that $P_v^{n,t}$ is regarded as positive during G2V operation and negative during V2G operation of EVs.

An EV, when connected to CS, can function as an energy storage unit that can operate in different operational modes: idle, uncoordinated G2V, and coordinated G2V/V2G mode. During idle mode, no power is exchanged between the EV and the CS, a condition that occurs when the EV is either fully charged or not connected to the CS. An uncoordinated mode represents the normal charging operation of an EV wherein it is charged at its rated power until it reaches its maximum SoC level. This operational method could potentially escalate peak energy demand with an increased number of EVs connected at CS. The coordinated G2V/V2G mode implements a controlled charging operation, aiming to alleviate grid burden by either lowering the aggregated energy demand of EVs at CS or by utilizing V2G operation to supply energy.

This study suggests a prioritization mechanism for the CSs, shown in Table I, to control the transition between various modes of EV operation. The proposed mechanism depends on two factors: the priority factor ($\rho_v^{n,t}$) and the pricing factor ($p_v^{n,t}$). A priority factor is derived from three key determinants: the SoC of the EV at the beginning of the interval, the necessary charging duration (\bar{t}_v^n) to reach the maximum SoC, and the departure time of the EV from the CS. The proposed priority factor is mathematically modeled as

$$\rho_v^{n,t} = (\overline{SoC} - SoC_v^{n,t})^{((t_{v,dep}^n - \bar{t}_v^n)/T)} \quad (3)$$

Algorithm 1 Pricing factor computational algorithm for EV

```

1: Initialize  $p_v^{n,t} = 0$ .
2: Initialize  $\mathcal{T} = \{i \mid \forall i \in [t, t_{v,dep}^n]\}$ .
3: Initialize  $\mathcal{Y} = \{\gamma^i \mid \forall i \in [t, t_{v,dep}^n]\}$ .
4: for  $i \in [1, t_{v,dep}^n - t]$  do
5:   for  $j \in [i + 1, t_{v,dep}^n - t + 1]$  do
6:     if  $\mathcal{Y}_i \geq \mathcal{Y}_j$  then
7:       Exchange the elements at the  $i^{th}$  index of  $\mathcal{Y}$  and  $\mathcal{T}$  with the elements at the  $j^{th}$  index.
8:     end if
9:   end for
10: end for
11: for  $i \in [1, \bar{t}_v^n]$  do
12:   if  $\mathcal{T}_i = t$  then
13:     Update  $p_v^{n,t} = 1$ 
14:   end if
15: end for
```

$$\text{where } \bar{t}_v^n = (\overline{SoC} - SoC_v^{n,t}) E_v^n / (\eta_{G2V} \overline{P}_v^n) \quad (3a)$$

As the priority factor of an EV increases from zero to unity, the necessity for charging the EV intensifies. A priority factor exceeding one indicates that the EV lacks sufficient parking time at CS to reach its maximum SoC and, therefore, cannot undergo coordinated charging. Thus, (3) explicitly determines the preferences of each EV owner in terms of their energy demand during the pre-scheduled parking duration.

Further, a binary pricing factor is incorporated into the mode selection mechanism to account for electricity prices. This factor prohibits EV charging during peak price periods, thereby minimizing EV charging expenses. **Algorithm 1** outlines the methodology to determine the binary pricing factor for an EV during each operational interval.

By leveraging the different operational modes inherent in EVs, the CSs, acting as an aggregator of EVs, connected to designated nodes within the distribution network can engage in DR programs by modifying their energy consumption pattern to reduce the dependency on the utility grid. In exchange, the CSs may receive incentives from the VPP operator in the form of discounted electricity prices, structured as

$$cost_{CS}^n = \sum_{t \in \mathcal{S}^T} \gamma^t \left(\sum_{v \in \mathcal{S}_V^n} P_v^{n,t} \Delta t \right), \quad \forall n \in \mathcal{S}^N \quad (4)$$

However, the V2G operation of EVs will result in battery degradation that can be calculated in the form of battery degradation cost as [49]

$$cost_{deg,v}^n = \sum_{t \in \mathcal{S}^T} \left((DoD_v^{n,t})^{1-b_d} - (DoD_v^{n,t-1})^{1-b_d} \right) (1 - \rho_v^{n,t}) c_b E_v^n / a_d, \quad \forall v \in \mathcal{S}_V^n; \quad n \in \mathcal{S}^N \quad (5)$$

$$\text{where } DoD_v^{n,t} = 1 - SoC_v^{n,t} \quad (5a)$$

C. Battery swapping station

In this work, a BSS has been incorporated alongside the solar-powered generating station to store surplus energy and

TABLE II
OPERATIONAL MODE SELECTION MECHANISM FOR BATTERY

$\rho_b^{n,t}$	≥ 1	Uncoordinated G2B mode ($z_b^{n,t} = 1$)		
	< 1	s^t	$\geq \sigma$	Coordinated G2B mode ($z_b^{n,t} = 0$)
		$< \sigma$	Coordinated B2G mode ($z_b^{n,t} = -1$)	

facilitate its use during night hours. The batteries in BSS can be represented mathematically in terms of its SoC as

$$SoC_b^{n,t} = \begin{cases} SoC_b^{n,t-1} + \eta_b \left(\frac{P_b^{n,t} \Delta t}{E_b^n} \right), & \text{if } t \neq t_{b,arr} \\ SoC_{b,swap}^n, & \text{if } t = t_{b,arr} \end{cases} \quad \forall b \in \mathcal{S}_B^n; \quad n \in \mathcal{S}^N; \quad t \in \mathcal{S}^T \quad (6)$$

$$\text{where } \eta_b = \begin{cases} \eta_{G2B}, & \text{if battery is in G2B mode} \\ 1/\eta_{B2G}, & \text{if battery is in B2G mode} \end{cases} \quad (6a)$$

Here, $P_b^{n,t}$ is regarded as positive during the G2B operation and negative during the B2G operation. An important point to note here is that the SoC of the battery, after the swapping operation, will transition to a different level, typically lower, based on the SoC ($SoC_{b,swap}^n$) of the EV's battery registered for the swapping operation at the time $t_{b,arr}^n$. Also, this work assumes that BSS is available for swapping operations in only daytime.

The batteries within the BSS can utilize the operational mode selection mechanism detailed in **Section II-B** with minor adjustments. Given that the BSS primarily functions to store surplus energy without drawing power from the grid for charging, pricing considerations are irrelevant in the mode selection mechanism for the battery. Instead, the mechanism should incorporate solar irradiance levels to facilitate G2B mode during day hours and B2G mode during night hours, as shown in **Table II**. The solar irradiance levels can determine the operating intervals when the solar is available for the scheduling operation and thus, makes it an important factor in determining the intervals for G2B and B2G mode operation.

Moreover, the BSS offers an alternative charging solution for EV users who opt out of participating in the DR program due to their limited parking durations. So, the priority factor of the battery will depend on the information of the EV registered for battery swapping and is calculated as

$$\rho_b^{n,t} = (\overline{SoC} - SoC_b^{n,t})^{((t_{b,arr}^n - t) - \bar{t}_b^n)/T} \quad (7)$$

$$\text{where } \bar{t}_b^n = (\overline{SoC} - SoC_b^{n,t}) E_b^n / (\eta_{G2B} \overline{P}_b^n) \quad (7a)$$

D. Controllable loads

Typically, energy consumers opt to engage in DR programs voluntarily, aiming to obtain benefits such as lower electricity expenses or incentives. These consumers can be analyzed based on their energy procurement costs from the utility grid, which can be expressed as

$$cost_{CL}^n = \sum_{t \in \mathcal{S}^T} \alpha^t (P_0^{n,t} - P_{shift}^{n,t}) \Delta t, \quad \forall n \in \mathcal{S}^L \quad (8)$$

Here, $P_{shift}^{n,t}$ is positive for the load curtailment and negative for load increment. Furthermore, to provide flexibility to

Algorithm 2 Pricing factor computational algorithm for controllable loads

```

1: Initialize  $p_{CL}^{n,t} = 0$ ; and  $T_0 = t_{stop}^n - t_{start}^n + 1$ .
2: Initialize  $\mathcal{T} = \{i \mid \forall i \in [t_{start}^n, t_{stop}^n]\}$ .
3: Initialize  $\mathcal{Y} = \{\alpha^i \mid \forall i \in [t_{start}^n, t_{stop}^n]\}$ .
4: for  $i \in [1, T_0 - 1]$  do
5:   for  $j \in [i + 1, T_0]$  do
6:     if  $\mathcal{Y}_i \leq \mathcal{Y}_j$  then
7:       Exchange the elements at the  $i^{th}$  index of  $\mathcal{Y}$  and  $\mathcal{T}$  with the elements at the  $j^{th}$  index.
8:     end if
9:   end for
10: end for
11: for  $i \in [1, T_0]$  do
12:   if  $\mathcal{T}_i = t$  then
13:     Update  $p_{CL}^{n,t} = 1$ ; and  $T_0 = T_0 - 1$ .
14:   end if
15: end for

```

consumers in terms of DR participation time, this work assumes that the consumers with controllable loads need to have advance registration of their preferred time slot $[t_{start}^n, t_{stop}^n]$ for load curtailments.

To lower the electricity expenses for these consumers, the VPP operator coordinates the usage of their controllable loads by adjusting them to intervals when electricity prices are low. This determination of low-priced intervals relies on a binary pricing factor determined by **Algorithm 2**. Thereafter, intervals, where the pricing factor is unity, are designated for load curtailment, while the remaining intervals are utilized for shifting the curtailed loads.

Further, the shifting of controllable loads may result in discomfort to consumers involved in the operation, which can be mathematically expressed in the form of discomfort cost as [50]

$$cost_{dis}^n = \sum_{t \in \mathcal{S}^T} \left(e^{\beta^n (p_{CL}^{n,t} P_{shift}^{n,t} / P_0^{n,t})} - 1 \right) \quad (9)$$

III. MULTI-OBJECTIVE PROBLEM FORMULATION

This section introduces the mathematical formulations of the proposed multi-objective VPP scheduling problem in a day-ahead market. For a better understanding, the deterministic formulation, ignoring the uncertainties in the scheduling problem, is provided in the first subsection. However, in the day-ahead market, uncertainties prevail regarding generation, load, and electricity prices, rendering them unknown. A stochastic model, using Hong's $(2m+1)$ PEM [48], is formulated in this work to consider these uncertainties, which is discussed in a later subsection.

A. Deterministic problem formulation

The proposed work considers VPP scheduling for a day-ahead market from the perspective of different stakeholders, i.e., EVs, CSs, controllable loads, VPP operators, and DS operators, involved in the VPP operation.

From the VPP operator's viewpoint, they aim to optimize profitability by meeting the demand of CSs using power from

solar generating stations. Any surplus solar energy can be stored in batteries located at BSS and subsequently supplied to the DS at a reduced electricity rate. The profit function of the VPP operator is mathematically modeled as

$$F_1 = \begin{cases} \sum_{n \in \mathcal{S}^N} \sum_{t \in \mathcal{S}^T} \gamma^t P_{inj}^{n,t} \Delta t, & \text{if } z_{inj}^{n,t} = 1 \\ \sum_{n \in \mathcal{S}^N} \sum_{t \in \mathcal{S}^T} \alpha^t P_{inj}^{n,t} \Delta t, & \text{if } z_{inj}^{n,t} = 0 \end{cases} \quad (10)$$

$$\text{where } P_{inj}^{n,t} = \left(P_s^{n,t} - \sum_{v \in \mathcal{S}_V^n} P_v^{n,t} - \sum_{b \in \mathcal{S}_B^n} P_b^{n,t} \right) \quad (10a)$$

However, the VPP also aims to establish a balanced approach in determining the appropriate scale for solar power generation facilities that aligns with their installation expenses. In mathematical terms, it can be articulated by considering daily capital investments alongside capital recovery factors and maintenance expenses, as expressed in (11).

$$F_2 = \sum_{n \in \mathcal{S}^N} (c_i c_p + c_0) P_s^n / 365 \quad (11)$$

$$\text{where capital recovery factor, } c_i = \frac{r(1+r)^L}{(1+r)^L - 1} \quad (11a)$$

Furthermore, the CSs and consumers with controllable loads, who are the key participants in the DR program, perceive the VPP scheduling problem as a chance to minimize their daily energy expenses. As elaborated in the preceding section, this study integrates incentivized electricity rates for CSs, while consumers with controllable loads gain advantages by adjusting their energy usage to periods of lower prices. Mathematically, the functional objective of DR participants is formulated as

$$F_3 = \sum_{n \in \mathcal{S}^N} cost_{CS}^n + \sum_{n \in \mathcal{S}^L} cost_{CL}^n \quad (12)$$

In the proposed DR program, the utilization of V2G technology could lead to unforeseen expenses related to battery degradation of EVs. Furthermore, consumers with controllable loads may experience inconvenience or discomfort as a result of load shifting, necessitating efforts to minimize such impacts. A mathematical representation of undesirable conditions arises due to the DR program being modeled in the form of a cost function as

$$F_4 = \sum_{n \in \mathcal{S}^N} \sum_{v \in \mathcal{S}_V^n} cost_{deg,v}^n + \sum_{n \in \mathcal{S}^L} cost_{dis}^n \quad (13)$$

The DS operator seeks to diminish reliance on the utility grid, a goal that can be quantified in terms of grid power consumption expenses as

$$F_5 = \sum_{t \in \mathcal{S}^T} \alpha^t P_{grid}^t \Delta t \quad (14)$$

Given the diverse and often conflicting goals of the various stakeholders engaged in the operation of the VPP, the proposed multi-objective optimization problem is formulated as

$$\text{Minimize}_{\chi} \{-F_1, F_2, F_3, F_4, F_5\} \quad (15)$$

where $\mathcal{X} \in \{P_v^{n,t}, P_b^{n,t}, P_s^n, P_{shift}^{n,t}, \gamma^t\}$ represents the set of decision variables for the proposed optimization problem.

However, due to the inherent conflict within defined objective functions, simultaneous optimization of the proposed VPP scheduling problem is unattainable. This study employs the utopia-tracking method introduced in [51] to address the conflicting nature of multi-objective functions by consolidating them into a normalized mono-objective function. This strategy facilitates attaining a trade-off Pareto optimal solution that closely aligns with utopia points. The utopia-tracking methodology involves normalizing the individual objective function by considering optimal and suboptimal solutions as

$$f_i = \begin{cases} \frac{(F_i - F_{i*})}{(F_i^* - F_{i*})}, & \text{if } F_i \text{ is to be minimized} \\ \frac{(F_i^* - F_i)}{(F_i^* - F_{i*})}, & \text{if } F_i \text{ is to be maximized} \end{cases} \quad (16)$$

Based on the normalized objectives obtained using the utopia-tracking approach, the deterministic form of the multi-objective function outlined in (15) is reformulated as

$$\underset{\mathcal{X}}{\text{Minimize}} \quad \mathcal{F} = \sum_{i=1}^5 w_i f_i \quad (17)$$

subject to

$$P_s \leq P_s^n \leq \overline{P}_s, \quad \forall n \in \mathcal{S}^N \quad (17a)$$

$$z_v^{n,t} \overline{P}_v^n \leq P_v^{n,t} \leq \overline{P}_v^n, \quad \forall n \in \mathcal{S}^N; v \in \mathcal{S}_V^n; t \in \mathcal{S}^T \quad (17b)$$

$$z_b^{n,t} \overline{P}_b^n \leq P_b^{n,t} \leq \overline{P}_b^n, \quad \forall n \in \mathcal{S}^N; b \in \mathcal{S}_B^n; t \in \mathcal{S}^T \quad (17c)$$

$$\mu_1 \alpha^t \leq \gamma^t \leq \mu_2 \alpha^t, \quad \forall t \in \mathcal{S}^T \quad (17d)$$

$$\underline{P}_{shift}^{n,t} \leq P_{shift}^{n,t} \leq \overline{P}_{shift}^{n,t}, \quad \forall n \in \mathcal{S}^L; t \in \mathcal{S}^T \quad (17e)$$

$$\underline{SoC} \leq SoC_v^{n,t} \leq \overline{SoC}, \quad \forall n \in \mathcal{S}^N; v \in \mathcal{S}_V^n; t \in \mathcal{S}^T \quad (17f)$$

$$\underline{SoC} \leq SoC_b^{n,t} \leq \overline{SoC}, \quad \forall n \in \mathcal{S}^N; b \in \mathcal{S}_B^n; t \in \mathcal{S}^T \quad (17g)$$

$$SoC_v^{n,t_{v,dep}} = \overline{SoC}, \quad \forall n \in \mathcal{S}^N; v \in \mathcal{S}_V^n \quad (17h)$$

$$SoC_b^{n,t_{b,arr}} = \overline{SoC}, \quad \forall n \in \mathcal{S}^N; b \in \mathcal{S}_B^n \quad (17i)$$

$$\sum_{t \in \mathcal{S}^T} P_{shift}^{n,t} = 0, \quad \forall n \in \mathcal{S}^L \quad (17j)$$

$$\sum_{t \in \mathcal{S}^T} p_{CL}^{n,t} P_{shift}^{n,t} \leq \lambda_1 \sum_{t \in \mathcal{S}^T} P_0^{n,t}, \quad \forall n \in \mathcal{S}^L \quad (17k)$$

$$\frac{\sum_{t \in \mathcal{S}^T} \alpha^t P_{shift}^{n_1,t}}{\sum_{t \in \mathcal{S}^T} \alpha^t P_{shift}^{n_2,t}} = \frac{cost_{dis}^{n_1}}{cost_{dis}^{n_2}}, \quad \forall \beta^{n_1} = \beta^{n_2}; n_1, n_2 \in \mathcal{S}^L \quad (17l)$$

$$P_s^{n,t} \geq \lambda_2 \left(\sum_{v \in \mathcal{S}_V^n} P_v^{n,t} + \sum_{b \in \mathcal{S}_B^n} P_b^{n,t} \right), \quad \forall n \in \mathcal{S}^N; t \in \mathcal{S}^T \quad (17m)$$

$$\sum_{n \in \mathcal{S}^N} \sum_{t \in \mathcal{S}^T} z_{inj}^{n,t} \gamma^t P_{inj}^{n,t} \Delta t \leq DB \quad (17n)$$

The operational constraints outlined in (17a)-(17e) delineate the boundary thresholds for various decision variables of the proposed optimization problem. The maximum capacity of a

solar station is determined by the extent of the sun-exposed area accessible to the operator, as outlined in (17a). The boundary limit of batteries within EVs and BSS are contingent upon their manufacturer-specified power ratings and is integrated into the problem using (17b) and (17c), respectively. However, a flag indicator is employed in the formulation to signify the transition between various operational modes in accordance with the priority mechanism outlined in the preceding section. Furthermore, the incentivized electricity rate offered by the VPP operator must consistently remain lower than the prevailing market electricity rate by the margins outlined in (17d). In this work, the value of μ_1 and μ_2 is fixed to 0.6 and 0.9, respectively. The power curtailment limits for consumers with controllable loads have been incorporated in the work using (17e). Considering the work presented in [52], this work assumes that sixty percent of loads in each operating interval are controllable. Further, to restrict the proposed DR program from forming another peak during an off-peak period, this work formulates the curtailment limits as

$$\overline{P}_{shift}^{n,t} = 0.6 P_0^{n,t}; \quad \underline{P}_{shift}^{n,t} = P_0^{n,t} - \overline{P}_0^n \quad (18)$$

To restrict the batteries from over-charging and over-discharging, constraints (17f) and (17g) ensure that the SoC of batteries within EVs and BSS are within the prescribed limits. Additionally, the operator must guarantee that EVs departing from the CS at their designated time and EVs enlisted for battery swapping receive batteries with the maximum SoC level. This assurance is achieved using (17h) and (17i), respectively.

Equation (17j) guarantees that consumers will not experience any reduction in load when calculated on a day scale. Furthermore, in this study, (17k) is implemented to ensure that the overall load shifts in a day remain within tolerable levels of discomfort for consumers. This work assumes that all consumers share an equal level of acceptable discomfort, and thus, λ_1 is set to 0.2. However, to maintain uniformity among consumers with controllable loads, the VPP operator must ensure that the benefits provided to consumers align proportionately with any inconvenience resulting from load control implemented by the VPP. This task is managed using (17l).

Further, when determining the ideal capacity for a solar-powered generating station, the VPP operator must address concerns regarding under-sizing, which could arise when minimizing the objective function F_2 . This condition is managed by introducing (17m) as an operating constraint that ensures the fulfillment of certain factors of CSs and BSSs demand during the daytime. Thus, in this work, λ_2 is assigned a value of 0.6 during daytime and 0 during nighttime. Finally, considering the limited daily budget of the DS operator, constraint (17n) restricts the financial transaction from the DS operator to the VPP operator.

B. Stochastic problem formulation

In the stochastic scenario, uncertain input variables are characterized by probabilistic information derived from their mean, standard deviation, and PDF. This work focuses on the uncertainties in the energy demand of DR participants, i.e.,

EVs and controllable loads, whose PDFs are considered to be a Gaussian distribution function, represented as

$$f_u = \frac{1}{\sigma_u \sqrt{2\pi}} \exp\left(-\frac{(u - \mu_u)^2}{2\sigma_u^2}\right), \forall u \in \mathcal{S}^U \quad (19)$$

Hong's $(2m+1)$ PEM uses this information to analytically define the different concentrations (or scenarios) in the form of locations, with their respective weights, of the uncertain input variables as [48]

$$p_{u,k} = \mu_u + \xi_{u,k} \sigma_u, \forall u \in \mathcal{S}^U; k = \{1, 2\}$$

$$\omega_{u,k} = \begin{cases} \frac{(-1)^{3-k}}{\xi_{u,k} \cdot (\xi_{u,1} - \xi_{u,2})}, & k = 1, 2 \\ \frac{1}{m} - \frac{1}{\lambda_{u,4} - (\lambda_{u,3})^2}, & k = 3 \end{cases} \quad (20)$$

where

$$\xi_{u,k} = \begin{cases} \frac{\lambda_{u,3}}{2} + (-1)^{3-k} \sqrt{\lambda_{u,4} - \frac{3}{4}(\lambda_{u,3})^2}, & k = 1, 2 \\ 0, & k = 3 \end{cases} \quad (20a)$$

$$\lambda_{u,j} = \frac{M_j(u)}{(\sigma_u)^j}, \forall j = \{1, 2, 3, 4\} \quad (20b)$$

$$M_j(u) = \int_{-\infty}^{\infty} (u - \mu_u)^j f_u du, \forall j = \{1, 2, 3, 4\} \quad (20c)$$

Using the various locations derived from Hong's $(2m+1)$ PEM, the deterministic problem outlined in (17) is evaluated for $(2m+1)$ iterations, each involving distinct values of the uncertain variables, as depicted by

$$\text{Minimize}_{\mathcal{X}} \mathcal{F}_{obj} = \sum_u \sum_k \omega_{u,k} \mathcal{F}(p_{u,k}, \mathcal{S}') \quad (21)$$

subject to (17a)-(17n).

Here, $\mathcal{S}' = \{\mu_i | i \in \mathcal{S}^U, i \neq u\}$. The proposed stochastic formulation aims to minimize the mean value of the multi-objective VPP scheduling problem. However, it can also be used to minimize the other probabilistic information of the scheduling problem.

IV. RESULTS AND VALIDATIONS

This section provides an overview of the input data for the proposed multi-objective VPP scheduling problem. Subsequent subsections discuss simulation results acquired from MATLAB and the real-time digital simulator (RTDS).

A. System data

The proposed problem is solved on a 12.66 kV, 33-node DS [53] with peak active and reactive power demands of 3715 kW and 2300 kVAr, respectively. The total power loss in the DS with the peak demand is calculated to be 202.67 kW. Further, different DER technologies explained in Section II are integrated at the optimal bus locations of the 33-node DS. However, to reduce DC-AC conversion losses, this work assumes the integration of solar stations, CSs, and BSSs at node numbers 8, 15, 21, 23, and 30 as a single unit, thus, forming solar-powered battery-integrated EV CSs at each node location. Further, it is presumed that each CS is outfitted with ten distinct models of EV chargers, with the

TABLE III
PROBABILISTIC INFORMATION OF EVS AND CONTROLLABLE LOADS

		Mean	Standard deviation	Min/Max
EV	Arrival time	08:00	03:00	01:00/20:00
	Departure time	17:00	03:00	11:00/24:00
	SoC at arrival	0.5	0.25	0.3/0.9
Controllable loads	DR start time	08:00	03:00	01:00/20:00
	DR stop time	17:00	03:00	11:00/24:00

TABLE IV
VALUES OF DIFFERENT PARAMETERS

Parameter	Value	Parameter	Value	Parameter	Value
Δt (h)	1	c_p (\$/kWp)	882.1	T	24
$\eta_{G2V/V2G}$	0.9	c_o (\$/kWp-year)	16.11	T_0 ($^{\circ}$ C)	41
$\eta_{G2B/B2G}$	0.9	DB (\$)	750	T_a ($^{\circ}$ C)	25
λ_1	0.2	k_v (%V/ $^{\circ}$ C)	0.27	V_{MPP} (V)	40.6
λ_2	0.6	k_i (%A/ $^{\circ}$ C)	0.05	V_{OC} (V)	48.8
a_d	1331	L^t (years)	30	I_{MPP} (A)	13.06
b_d	-1.825	$P_{s,rated}$ (W)	530	I_{SC} (A)	13.8
c_b (\$/kWh)	323.18	r (%)	10		

capacity to accommodate 100 EVs daily. Detailed technical specifications for the ten EV models under consideration can be found in [23]. The uncertainty in the arrival and departure schedules of EVs at the CSs is addressed by utilizing the data provided in Table III. Additionally, to ensure the availability of the appropriate battery for each type of EV during the swapping operation at the BSS, ten batteries with matching specifications to those of EV batteries are stocked at the BSS. Furthermore, to determine the optimal size for solar-powered generating stations, this study takes into account the technical specifications and cost information of solar modules provided in [54].

This work also assumes the participation of all consumers of the DS in the DR program, focusing on various consumer categories such as residential, commercial, and industrial, with more details available in [55]. A standard deviation of 2% is incorporated into the hourly energy demands of consumers to account for their variability. Additionally, the start and stop times for their DR operations are determined based on probabilistic data provided in Table III. Other important parameters considered in this study are tabulated in Table IV and are available in [23].

B. Simulation results

The proposed VPP scheduling optimization problem is addressed utilizing an improved Jaya algorithm, the algorithm of which is available in [23]. The simulation work is performed using MATLAB R2023b on a desktop equipped with an Intel Core i9-14900K 3.20 GHz CPU and 64GB of memory.

The problem proposed in this paper is framed as a conflicting multi-objective optimization problem, reflecting the inherent conflicts arising from the differing perspectives of the stakeholders involved in the VPP operation. The inherent conflicts within a multi-objective problem limit the ability of the VPP operator to attain optimal solutions for

TABLE V
UTOPIA, NADIR AND OPTIMIZED VALUE OF MULTI-OBJECTIVE PROBLEM

Objectives	F_1	F_2	F_3	F_4	F_5
Utopia point	689.28	975.85	5027.33	28.14	3831.04
Nadir point	290.89	1455.35	5282.67	875.94	4535.38
Optimized point	636.71	1060.32	5092.59	179.67	4088.68

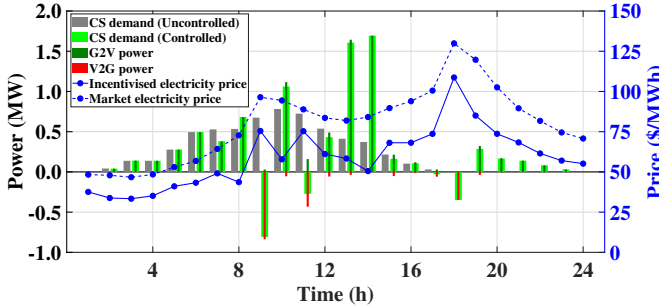


Fig. 2. Hourly CS energy demand and incentivized electricity price for a day.

all stakeholders. Consequently, this study employs a utopia-tracking approach to strive for a near-optimal solution for each objective of the proposed problem. The utopia-tracking approach relies on identifying hyperparameters, which include defining the utopia and nadir points. The advantage of the utopia-tracking approach is that the hyperparameters can be calculated offline and processed in parallel. Moreover, the utopia-tracking approach does not necessitate the computation of the entire Pareto front, constituting a significant advantage over existing multi-objective problem-solving methods. The offline-calculated values of the utopia and nadir points for the various objectives are presented in **Table V**. Additionally, **Table V** includes the near-optimal values of each objective, which are close to the utopia points.

The primary aim of the proposed work is to establish an efficient approach for controlling the charging operation of EVs at the CS, taking into account the individual priorities of each EV user. **Figure 2** illustrates the daily distribution of hourly energy demand from CS, showcasing the efficient utilization of EVs as storage units during controlled G2V/V2G operations in contrast to their uncontrolled operations. The VPP operator offers an incentivized electricity price to encourage the participation of CSs in the DR program, which is depicted in **Fig. 2** and is notably lower than the prevailing market electricity price. The proposed incentive strategy ensures that EVs conduct G2V operations during periods of low pricing and V2G operations during high pricing periods. Additionally, the strategy guarantees that EVs achieve the maximum SoC feasible upon departure, as evidenced by the SoC depicted in the candlestick chart presented in **Fig. 3**, illustrating the status of 100 EVs at the CS integrated into node number 8.

Consumers possessing controllable loads, integrated at various nodes of the DS, actively engage in the DR program by adjusting their load operation schedules to coincide with low-price periods and, thus, are rewarded by the reduced electricity bill for a day operation. **Figure 4** illustrates the

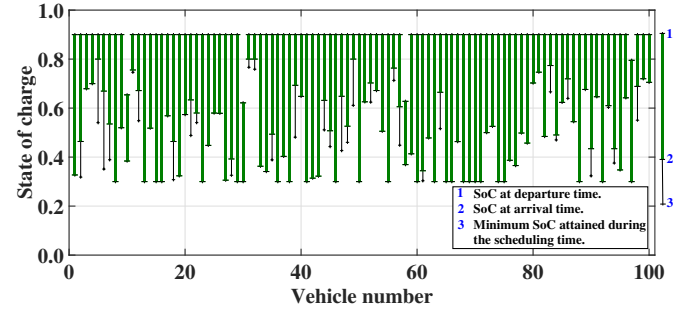


Fig. 3. Variation in SOC of EVs during their stay at the CS.

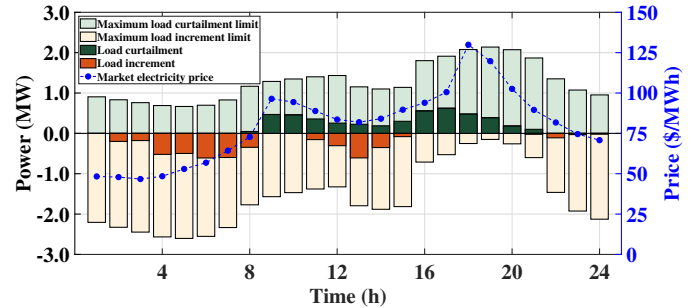


Fig. 4. Hourly load curtailments and increments for the consumers with controllable loads.

overall energy adjustment within each operational interval, highlighting instances of load reduction during periods of peak pricing. It also verifies the successful establishment of boundary limits for load shifting during any operational interval, aiming to prevent the occurrence of another peak in the off-peak period.

Further, the proposed VPP scheduling approach recommends the optimal size for the solar-powered generating station to maximize the satisfaction of energy requirements for CSs and BSSs through the renewable source, illustrated in **Fig. 5**. **Figure 5** also confirms the power demand and supply balance in the VPP framework achieved by taking advantage of V2G and B2G operation of EVs and batteries as a power source at each operating interval. The surplus solar energy is stored within the batteries at the BSS to be utilized by CSs during night hours. Additionally, following the satisfaction of the energy demands of CSs and BSSs, the suggested scheduling approach further enhances the profitability of the VPP by supplying electricity to DS at incentivized pricing. The quantitative measure of the total energy supplied by the VPP to the DS during a day, along with the corresponding profit generated from this energy transaction is shown in **Table VI**.

Table VI also demonstrates improvements in the energy reliance of DS on the grid and the energy dissipated in the distribution network. Additionally, it presents advancements in the operational costs for various stakeholders. Furthermore, this study effectively addresses the impact of uncertain energy demands from controllable loads and CSs, which is presented in terms of mean and standard deviations in energy and cost shown in **Table VI**.

A set of scenarios has been generated using Hong's (2m+1)

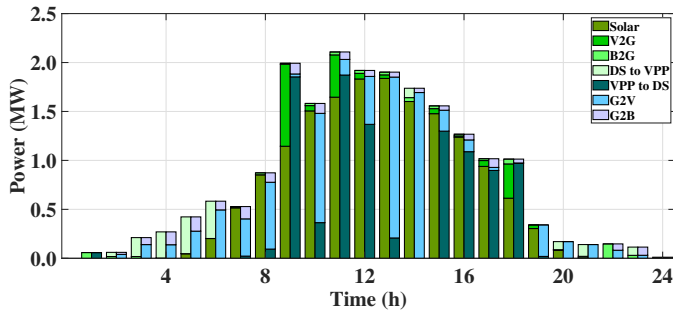


Fig. 5. Hourly power exchange between solar, EVs, batteries, and DS as a source and load within the VPP framework.

TABLE VI
COMPARISON OF THE PROPOSED APPROACH WITH THE UNCONTROLLED APPROACH IN A DAY-AHEAD OPERATION

	Uncontrolled Approach	Proposed Approach	% reduction
Energy purchased from the grid (MWh)	67.97 (0.84)	53.70 (2.35)	20.99
Energy delivered by the VPP to the DS (MWh)	-	10.43 (0.58)	-
Energy lost in the DS (MWh)	2.5314 (0.0517)	1.9637 (0.1067)	22.43
Cost of energy purchased from the grid (\$)	5614.14 (80.44)	4116.38 (167.15)	26.68
VPP profit made by delivering energy to the DS (\$)	-	583.72 (109.37)	-
Cost of charging EVs (\$)	411.63 (76.47)	269.94 (68.06)	34.42
Electricity cost of consumers with controllable loads (\$)	4949.36 (7.62)	4786.96 (22.10)	3.28

Blue and Red colour represent the mean and standard deviation, respectively.

PEM to model the uncertainty in arrival and departure time of EVs at CSs, as well as the stochastic SoC upon their arrival. Additionally, scenarios have been developed to represent the varying load demand of consumers with controllable loads. A total of $(2m+1)$ scenarios were generated and analyzed within the framework of the proposed VPP scheduling problem. The scheduling problem is optimized using various variables, with their stochastic behavior at each operational interval depicted through the boxplot in Fig. 6. The boxplots presented in Fig. 6a indicate that the power demand of EVs at CSs in each scenario decreases during high electricity prices. Additionally, the CSs enable V2G operations when necessary, supporting the VPP operator in reducing reliance on the grid during these high-price periods. Similar observations can be made for the controllable loads and BSSs from the boxplots illustrated in Fig. 6b and Fig. 6c, respectively. Further, Fig. 6d illustrates that the incentivized pricing rate defined by the VPP operator in each scenario adheres to the generalized rules outlined in the operational guidelines. This structure encourages consumers to engage in the DR program by modifying their energy consumption pattern or participating in V2G operations during peak pricing periods to receive generous incentives.

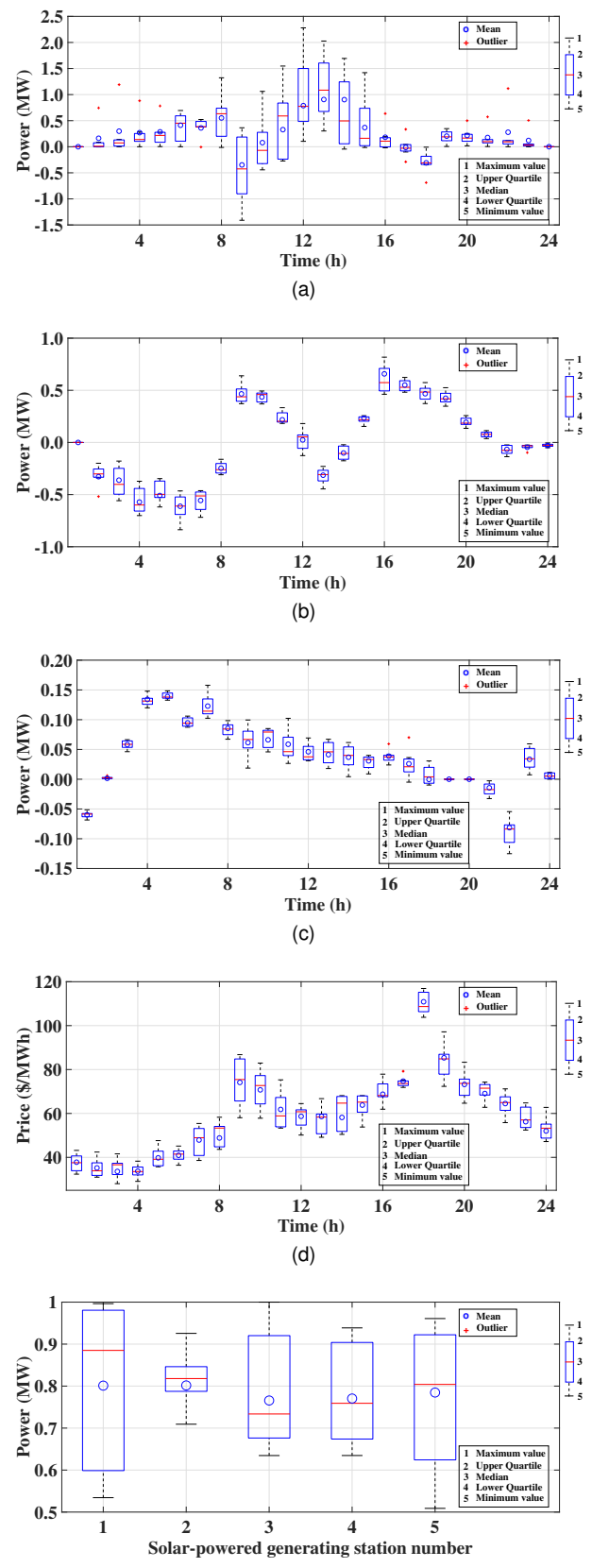


Fig. 6. Boxplot representation for stochastic optimization variables i.e. (a) aggregated CS power demand; (b) aggregated load shift of controllable loads; (c) aggregated BSS power demand; (d) incentivized electricity price rate; & (e) capacity of the solar-powered generating station.

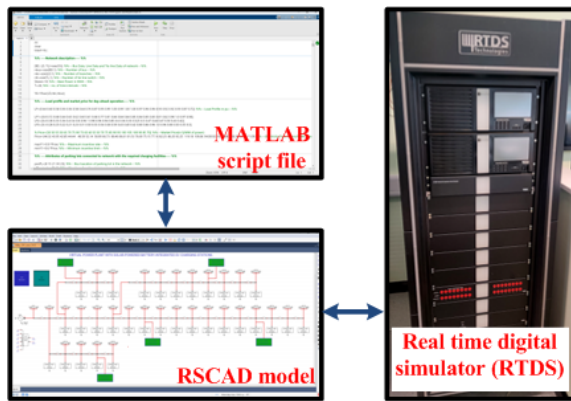


Fig. 7. Software-in-loop setup with MATLAB, RSCAD and RTDS.

Furthermore, each scenario illustrates the capacity of the solar-powered generating stations integrated within the CSs, as statistically represented through the boxplot in **Fig. 6e**.

C. Result validation

A software-in-the-loop simulation utilizing MATLAB, RSCAD, and RTDS is conducted to validate the accuracy and efficacy of the proposed VPP scheduling methodology. It is important to note here that this study employs the conventional Newton-Raphson power flow technique for determining the voltages at each node within the DS. The Newton-Raphson method addresses the linearized power flow model derived from approximating the non-linear power flow equations. However, this approximation can potentially result in overestimation or underestimation of node voltage values, thereby posing a risk to the accuracy of the results. Thus, in this work, the VPP network comprising DS, CS, BSS, and solar-powered generating stations is first modeled in RSCAD, followed by real-time EMT simulation executed in RTDS, where non-linear differential equations associated with the VPP model are solved at each time-step (typically within $50\mu s$) so that this simulation is free from the errors due to the linear approximations.

The MATLAB and RSCAD-RTDS co-simulation platform, as shown in **Fig. 7**, is developed using the logical and physical ports of the Gigabit transceiver network communication (GTNETx2) card, which is installed in the RTDS rack. The GTNETx2 card provides support for the TCP/IP Socket protocol, allowing for bidirectional communication between MATLAB and RSCAD-RTDS. This capability enables the transmission and reception of stored real-time network variable data from RSCAD to MATLAB, as well as from MATLAB to RSCAD, at every 1s interval.

The software-in-loop simulation validates that the DS operates without transients during each operational interval. The nodes most susceptible to vulnerabilities, which are integrated with CSs and serve as common points for energy exchange between VPP and DS, have been chosen to showcase the transient-free voltage waveform depicted in **Fig. 8**. Further, from the **Fig. 5**, it is concluded that the maximum energy exchange between the VPP and DS occurs during the eleventh hour of the day, indicating this period as a potential operational

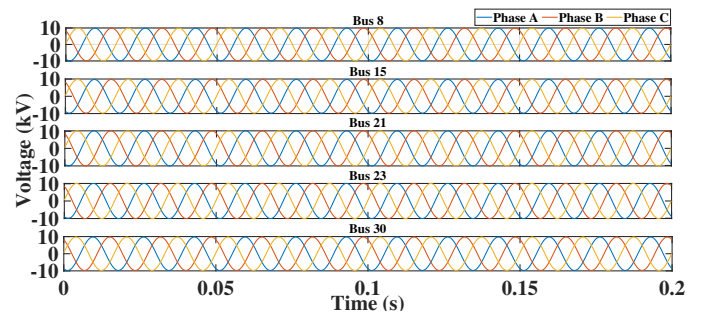


Fig. 8. Node voltage of CSs at the Hour 11.

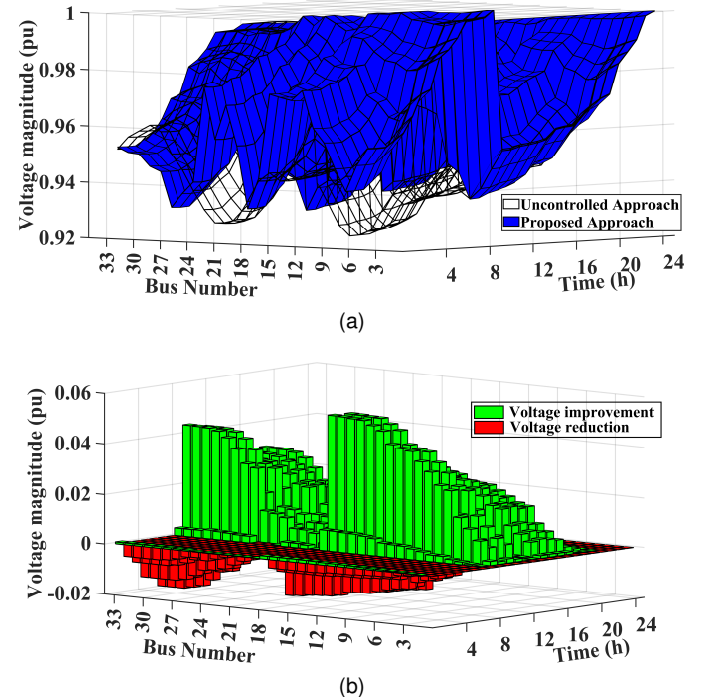


Fig. 9. (a) Hourly voltage profile, & (b) Voltage improvement obtained in the proposed approach compared to the uncontrolled approach.

interval with transients. However, **Fig. 8** validates the steady operation of DS at the eleventh hour of the day. Further, the improvement in the voltage profile of all the nodes in DS, particularly during day hours, is showcased in **Fig. 9**. The night hours experience some reduction in the voltages due to the load-shifting operation during the low-price period. It also confirms that the node voltage limits (typically $\pm 5\%$) were not violated during the operation of the DS. However, the proposed scheduling approach is focused more on the economic aspects rather than the technical aspects associated with the DS. So, the voltage improvements can only be considered an indirect benefit of the VPP scheduling approach on the DS with the DER models under the test conditions considered for this work.

V. CONCLUSION

A stochastic priority-ordered incentive-based DR program is presented in this work for the effective energy scheduling in the VPP comprised of solar-powered generating stations, BSSs, EV CSs, and consumers with controllable loads. The

priority mechanism is suggested for the EVs at different CSs to effectively utilize the EVs as a storage unit in the VPP scheduling approach while ensuring the attainment of maximum SoC at their departure time. A multi-objective VPP scheduling problem is presented in this work to account for the conflicting objectives of different stakeholders and a utopia-tracking approach is used to find a near-optimal solution for each objective. Further, the incentives offered by the VPP operator at the end of scheduling lead to the reduction in the charging cost of EVs by 34.42% and the electricity cost of consumers with controllable loads by 3.28%. The simulation results verify that all the operational constraints are satisfied during the operation. Furthermore, the co-simulation using RSCAD-RTDS validates the steady-state operation of DS in each operating interval. Future work will focus on increasing the resiliency of the VPP operation during unexpected or undesirable weather conditions.

REFERENCES

- [1] "World energy trilemma index," World Energy Council, London, UK, Tech. Rep., 2022. [Online]. Available: https://www.worldenergy.org/assets/downloads/World_Energy_Trilemma_Index_2022.pdf
- [2] "Distributed energy resources: Connection modeling and reliability considerations," North American Electric Reliability Corporation, Atlanta, USA, Tech. Rep., 2017. [Online]. Available: https://www.nerc.com/comm/Other/essntrllbtltsrvestskfrcDL/Distributed_Energy_Resources_Report.pdf
- [3] D.-m. Han and J.-h. Lim, "Smart home energy management system using IEEE 802.15.4 and zigbee," *IEEE Transactions on Consumer Electronics*, vol. 56, no. 3, pp. 1403–1410, 2010.
- [4] R. Zafar, A. Mahmood, S. Razzaq, W. Ali, U. Naeem, and K. Shehzad, "Prosumer based energy management and sharing in smart grid," *Renewable and Sustainable Energy Reviews*, vol. 82, pp. 1675–1684, 2018.
- [5] F. Lezama, J. Soares, B. Canizes, and Z. Vale, "Flexibility management model of home appliances to support DSO requests in smart grids," *Sustainable Cities and Society*, vol. 55, p. 102048, 2020.
- [6] H. Gerard, E. I. Rivero Puente, and D. Six, "Coordination between transmission and distribution system operators in the electricity sector: A conceptual framework," *Utilities Policy*, vol. 50, pp. 40–48, 2018.
- [7] K. Christakou, "A unified control strategy for active distribution networks via demand response and distributed energy storage systems," *Sustainable Energy, Grids and Networks*, vol. 6, pp. 1–6, 2016.
- [8] Y. Xie, Y. Zhang, W.-J. Lee, Z. Lin, and Y. A. Shamash, "Virtual power plants for grid resilience: A concise overview of research and applications," *IEEE/CAA Journal of Automatica Sinica*, vol. 11, no. 2, pp. 329–343, 2024.
- [9] J. Shah, "Introducing VPPieces: Bite-sized blogs about virtual power plants," Loan Program Office, U.S. Department of Energy, Washington D.C., U.S., Tech. Rep., 2022. [Online]. Available: <https://www.energy.gov/lpo/articles/introducing-vppieces-bite-sized-blogs-about-virtual-power-plants>
- [10] A. Bonfiglio, S. Bruno, M. Martino, M. Minetti, R. Procopio, and A. Velini, "Renewable energy communities virtual islanding: A novel service for smart distribution networks," in *2024 IEEE/IAS 60th Industrial and Commercial Power Systems Technical Conference (I&CPS)*, 2024, pp. 1–8.
- [11] T. Morstyn, N. Farrell, S. J. Darby, and M. D. McCulloch, "Using peer-to-peer energy-trading platforms to incentivize prosumers to form federated power plants," *Nature Energy*, vol. 3, no. 2, pp. 94–101, 2018.
- [12] Y. Kuang, X. Wang, H. Zhao, T. Qian, N. Li, J. Wang, and X. Wang, "Model-free demand response scheduling strategy for virtual power plants considering risk attitude of consumers," *CSEE Journal of Power and Energy Systems*, vol. 9, no. 2, pp. 516–528, 2023.
- [13] H. Liang and J. Ma, "Data-driven resource planning for virtual power plant integrating demand response customer selection and storage," *IEEE Transactions on Industrial Informatics*, vol. 18, no. 3, pp. 1833–1844, 2022.
- [14] W. Zhong, M. A. A. Murad, M. Liu, and F. Milano, "Impact of virtual power plants on power system short-term transient response," *Electric Power Systems Research*, vol. 189, p. 106609, 2020.
- [15] S. K. Venkatachary, A. Alagappan, and L. J. B. Andrews, "Cybersecurity challenges in energy sector (virtual power plants) - can edge computing principles be applied to enhance security?" *Energy Informatics*, vol. 4, no. 1, pp. 5–26, 2021.
- [16] J. Deng and Q. Guo, "Decentralized energy management system of distributed energy resources as virtual power plant: Economic risk analysis via downside risk constraints technique," *Computers & Industrial Engineering*, vol. 183, p. 109522, 2023.
- [17] X. Wang, H. Zhao, H. Lu, Y. Zhang, Y. Wang, and J. Wang, "Decentralized coordinated operation model of VPP and P2H systems based on stochastic-bargaining game considering multiple uncertainties and carbon cost," *Applied Energy*, vol. 312, p. 118750, 2022.
- [18] K. Heussen, S. You, B. Biegel, L. H. Hansen, and K. B. Andersen, "Indirect control for demand side management - a conceptual introduction," in *2012 3rd IEEE PES Innovative Smart Grid Technologies Europe*, 2012, pp. 1–8.
- [19] D. Papadaskalopoulos, G. Strbac, P. Mancarella, M. Aunedi, and V. Stanojevic, "Decentralized participation of flexible demand in electricity markets—Part II: Application with electric vehicles and heat pump systems," *IEEE Transactions on Power Systems*, vol. 28, no. 4, pp. 3667–3674, 2013.
- [20] M. Roozbehani, M. A. Dahleh, and S. K. Mitter, "Volatility of power grids under real-time pricing," *IEEE Transactions on Power Systems*, vol. 27, no. 4, pp. 1926–1940, 2012.
- [21] K. Margellos and S. Oren, "Capacity controlled demand side management: A stochastic pricing analysis," *IEEE Transactions on Power Systems*, vol. 31, no. 1, pp. 706–717, 2016.
- [22] M. Muratori, "Impact of uncoordinated plug-in electric vehicle charging on residential power demand," *Nature Energy*, vol. 3, no. 3, pp. 193–201, 2018.
- [23] P. Harsh and D. Das, "A priority-ordered incentive-based smart charging strategy of electric vehicles to determine the optimal size of solar power plant at the charging stations," in *2023 IEEE International Conference on Environment and Electrical Engineering and 2023 IEEE Industrial and Commercial Power Systems Europe*, 2023, pp. 1–6.
- [24] S. Sadeghi, H. Jahangir, B. Vatandoust, M. A. Golkar, A. Ahmadian, and A. Elkamel, "Optimal bidding strategy of a virtual power plant in day-ahead energy and frequency regulation markets: A deep learning-based approach," *International Journal of Electrical Power & Energy Systems*, vol. 127, p. 106646, 2021.
- [25] D. Yang, S. He, M. Wang, and H. Pandžić, "Bidding strategy for virtual power plant considering the large-scale integrations of electric vehicles," *IEEE Transactions on Industry Applications*, vol. 56, no. 5, pp. 5890–5900, 2020.
- [26] F. Sheidaei and A. Ahmarniajed, "Multi-stage stochastic framework for energy management of virtual power plants considering electric vehicles and demand response programs," *International Journal of Electrical Power & Energy Systems*, vol. 120, p. 106047, 2020.
- [27] "Handbook of electric vehicle charging infrastructure implementation," NITI Aayog, India, Tech. Rep., 2021. [Online]. Available: <http://www.niti.gov.in/sites/default/files/2021-08/HandbookforEVChargingInfrastructureImplementation081221.pdf>
- [28] H. Wang, Y. Jia, M. Shi, C. S. Lai, and K. Li, "A mutually beneficial operation framework for virtual power plants and electric vehicle charging stations," *IEEE Transactions on Smart Grid*, vol. 14, no. 6, pp. 4634–4648, 2023.
- [29] J. Wang, C. Guo, C. Yu, and Y. Liang, "Virtual power plant containing electric vehicles scheduling strategies based on deep reinforcement learning," *Electric Power Systems Research*, vol. 205, p. 107714, 2022.
- [30] S. Fan, J. Liu, Q. Wu, M. Cui, H. Zhou, and G. He, "Optimal coordination of virtual power plant with photovoltaics and electric vehicles: A temporally coupled distributed online algorithm," *Applied Energy*, vol. 277, p. 115583, 2020.
- [31] B. Zhou, K. Zhang, K. W. Chan, C. Li, X. Lu, S. Bu, and X. Gao, "Optimal coordination of electric vehicles for virtual power plants with dynamic communication spectrum allocation," *IEEE Transactions on Industrial Informatics*, vol. 17, no. 1, pp. 450–462, 2021.
- [32] C. Pape, "The impact of intraday markets on the market value of flexibility — decomposing effects on profile and the imbalance costs," *Energy Economics*, vol. 76, pp. 186–201, 2018.
- [33] N. Pearre and L. Swan, "Combining wind, solar, and in-stream tidal electricity generation with energy storage using a load-perturbation control strategy," *Energy*, vol. 203, p. 117898, 2020.
- [34] M. Song and M. Amelin, "Purchase bidding strategy for a retailer with flexible demands in day-ahead electricity market," *IEEE Transactions on Power Systems*, vol. 32, no. 3, pp. 1839–1850, 2017.

- [35] L. V. White and N. D. Sintov, "Inaccurate consumer perceptions of monetary savings in a demand-side response programme predict programme acceptance," *Nature Energy*, vol. 3, no. 12, pp. 1101–1108, 2018.
- [36] M. Eissa, "First time real time incentive demand response program in smart grid with "i-energy" management system with different resources," *Applied Energy*, vol. 212, pp. 607–621, 2018.
- [37] A. Mnatsakanyan and S. W. Kennedy, "A novel demand response model with an application for a virtual power plant," *IEEE Transactions on Smart Grid*, vol. 6, no. 1, pp. 230–237, 2015.
- [38] S. Yu, F. Fang, Y. Liu, and J. Liu, "Uncertainties of virtual power plant: Problems and countermeasures," *Applied Energy*, vol. 239, pp. 454–470, 2019.
- [39] L. Ju, R. Zhao, Q. Tan, Y. Lu, Q. Tan, and W. Wang, "A multi-objective robust scheduling model and solution algorithm for a novel virtual power plant connected with power-to-gas and gas storage tank considering uncertainty and demand response," *Applied Energy*, vol. 250, pp. 1336–1355, 2019.
- [40] D. Koraki and K. Strunz, "Wind and solar power integration in electricity markets and distribution networks through service-centric virtual power plants," *IEEE Transactions on Power Systems*, vol. 33, no. 1, pp. 473–485, 2018.
- [41] S. Fan, Q. Ai, and L. Piao, "Fuzzy day-ahead scheduling of virtual power plant with optimal confidence level," *IET Generation, Transmission & Distribution*, vol. 10, no. 1, pp. 205–212, 2016.
- [42] M. Riaz, S. Ahmad, I. Hussain, M. Naeem, and L. Mihet-Popa, "Probabilistic optimization techniques in smart power system," *Energies*, vol. 15, no. 3, 2022.
- [43] C. Wang, C. Liu, F. Tang, D. Liu, and Y. Zhou, "A scenario-based analytical method for probabilistic load flow analysis," *Electric Power Systems Research*, vol. 181, p. 106193, 2020.
- [44] E. I. Batzelis, G. E. Kampitsis, and S. A. Papathanassiou, "Power reserves control for PV systems with real-time MPP estimation via curve fitting," *IEEE Transactions on Sustainable Energy*, vol. 8, no. 3, pp. 1269–1280, 2017.
- [45] M. A. Tajeddini, A. Rahimi-Kian, and A. Soroudi, "Risk averse optimal operation of a virtual power plant using two stage stochastic programming," *Energy*, vol. 73, pp. 958–967, 2014.
- [46] M. Aien, A. Hajebrahimi, and M. Fotuhi-Firuzabad, "A comprehensive review on uncertainty modeling techniques in power system studies," *Renewable and Sustainable Energy Reviews*, vol. 57, pp. 1077–1089, 2016.
- [47] H. Hong, "An efficient point estimate method for probabilistic analysis," *Reliability Engineering & System Safety*, vol. 59, no. 3, pp. 261–267, 1998.
- [48] A. G. Zamani, A. Zakariazadeh, and S. Jadid, "Day-ahead resource scheduling of a renewable energy based virtual power plant," *Applied Energy*, vol. 169, pp. 324–340, 2016.
- [49] A. Kavousi-Fard, T. Niknam, and M. Fotuhi-Firuzabad, "Stochastic reconfiguration and optimal coordination of V2G plug-in electric vehicles considering correlated wind power generation," *IEEE Transactions on Sustainable Energy*, vol. 6, no. 3, pp. 822–830, 2015.
- [50] M. Yu and S. H. Hong, "A real-time demand-response algorithm for smart grids: A stackelberg game approach," *IEEE Transactions on Smart Grid*, vol. 7, no. 2, pp. 879–888, 2016.
- [51] V. M. Zavala and A. Flores-Tlacuahuac, "Stability of multiobjective predictive control: A utopia-tracking approach," *Automatica*, vol. 48, no. 10, pp. 2627–2632, 2012.
- [52] A. Soroudi, P. Siano, and A. Keane, "Optimal DR and ESS scheduling for distribution losses payments minimization under electricity price uncertainty," *IEEE Transactions on Smart Grid*, vol. 7, no. 1, pp. 261–272, 2016.
- [53] M. Baran and F. Wu, "Network reconfiguration in distribution systems for loss reduction and load balancing," *IEEE Transactions on Power Delivery*, vol. 4, no. 2, pp. 1401–1407, 1989.
- [54] V. Ramasamy, J. Zuboy, D. Feldman, R. Margolis, J. Desai, A. Walker, M. Woodhouse, E. O'Shaughnessy, and P. Basore, "Q1 2023 U.S. solar photovoltaic system and energy storage cost benchmarks with minimum sustainable price analysis data file," *NREL Data Catalog. Golden, CO: National Renewable Energy Laboratory*, 2023.
- [55] R. Hasanzpour, B. M. Kalesar, J. B. Noshahr, and P. Farhadi, "Reconfiguration of smart distribution network considering variation of load and local renewable generation," in *2017 IEEE International Conference on Environment and Electrical Engineering and 2017 IEEE Industrial and Commercial Power Systems Europe*, 2017, pp. 1–5.

Pratik Harsh received a Bachelor of Technology in Electrical and Electronics Engineering from the National Institute of Science and Technology Berhampur, Odisha, India, in 2014, a Master of Technology in Electrical Engineering from the National Institute of Technology Silchar, Assam, India, in 2017, and a Doctor of Philosophy in Electrical Engineering from Indian Institute of Technology Kharagpur, West Bengal, India in 2024. He is working as a Postdoctoral Research Associate with the Department of Engineering at Durham University, United Kingdom. He is working on different UKRI-funded projects that align with his research interests in AI-based energy management in microgrids and virtual power plants integrated with electric vehicles, solar, and other distributed energy resources.

Hongjian Sun received his Ph.D. degree in Electronics and Electrical Engineering at the University of Edinburgh (U.K.) and then took postdoctoral positions at King's College London (U.K.) and Princeton University (USA). Since April 2013, he has been with the Department of Engineering at the University of Durham, U.K. He is a Professor (Chair), a Chartered Engineer, a Fellow of Durham Energy Institute, and a Fellow of Higher Education Academy.

Prof. Sun is the Head of Durham Smart Grid Laboratory, leading a research team consisting of over 20 doctorate researchers. His research activities focus on (i) demand side management and demand response, and (ii) renewable energy sources integration and virtual power plants. He has an established track record of publishing high-quality scientific articles, with over 180 papers in refereed journals and international conferences.

Debapriya Das received the B.E. degree in electrical engineering from Calcutta University, Kolkata, India, the M.Tech. degree from the Indian Institute of Technology (I.I.T.) Kharagpur, Kharagpur, India, and the Ph.D. degree from I.I.T. Delhi. He is currently a Professor with the Department of Electrical Engineering, I.I.T. Kharagpur. His research interests include autonomous power generation systems, microgrids, and electrical power distribution systems.

Awagan Goyal Rameshrao received her B.Tech degree in Electrical Engineering from GCOE, Amravati, India, in 2013 and M.E degree in Electrical Power Systems from GEC, Aurangabad, India in 2016. She received her Ph.D degree in Electrical Engineering from the National Institute of Technology, Raipur, India in 2024. She is currently working as a Postdoctoral Research Fellow in the Department of Mathematics, Physics & Electrical Engineering at the University of Northumbria at Newcastle, UK. Her research interests include microgrid protection, cyber-physical systems, and the application of artificial intelligence to power systems. She is presently involved in two UKRI-funded projects i.e., VPP-WARD and SustainAIRAG6.

Jing Jiang is an Associate Professor and Head of Subject (Electrical Engineering) in the Department of Mathematics, Physics & Electrical Engineering at the University of Northumbria at Newcastle, UK. She received her Ph.D. degree in Electrical and Electronics Engineering from the University of Edinburgh in 2011. From 2011 to 2018, she took postdoctoral positions at the University of Surrey and then at Durham University, UK. Her relevant research interests include AI and Digital Twins in Future Energy Systems, Communication Technologies for Smart Grids, Data-driven Energy Scheduling, and Decarbonisation. She is now a Subject Editor of the IET Smart Grid Journal.